Polymer Bulletin 40, 283–290 (1998)

Polymer Bulletin

Mechanical behavior at low strain of microgel containing elastomers

A. Bischoff, M. Klüppel, R. H. Schuster

Deutsches Institut für Kautschuktechnologie e. V., Eupener Strasse 33, D-30519 Hannover, Germany

Received: 19 December 1997/Revised version: 7 January 1998/Accepted: 7 January 1998

Summary
Synthetic routes for the preparation of microgels with defined particle size, crosslinking density and surface chemistry are described. The mechanical effects caused by incorporating such systems in crosslinked rubber (NR and SBR) are described. The mechanical effects are qualitatively related to the state of clustering which is governed by the particle size and the interfacial tension (δ-parameter difference). The reinforcing effects on Young's modulus and the dynamic shear modulus are explained against a comprehensive theoretical background which assumes kinetically controlled cluster-cluster aggregation (CCA) of colloidal filler particles dispersed in entangled polymers. This leads to a control of rubber material properties by chemical means.

Introduction

The demand for a diversified property set for elastomers is generally fulfilled by mechanically blended rubbers with a specific chemical nature or microstructure and by reinforcing them using colloidal filler particles. The compatibility of polymers usually leads to heterogeneous phase morphologies, and is also strongly affected by the processing conditions and coalescence during intermediate storage of the blends. Because it is proven that phase morphology affects to some extent the physical properties these influences may result in changes of the product quality. In order to avoid this one can follow new approaches by using, as a blend constituent, (i) polymeric microgels with defined particle sizes, chemical nature, surface functionalization and monitored crosslinking densities [1,2] or (ii) core-shell systems with both variable core-size and adjustable chain length of the shell phase [3,4]. Not only do such systems show improved physico-chemical properties like high fuel resistance and reduced gas permeation, they also demonstrate unexpected mechanical properties which cannot be achieved with conventional unfilled rubber blends.

The aim of this paper is to describe the mechanical properties of microgel containing elastomers which are generated by (i) purely hydrodynamic contributions, (ii) cluster formation and (iii) formation of percolating microgel networks. It will be demonstrated that the property spectrum is controlled by the particular interfacial tension governing the system. The behavior can be described by cluster aggregation models of colloidal particles dispersed in

entangled polymers recently developed [5,6]. For this purpose three different types of microgels with specific Tg's, crosslinking densities and states of surface functionalization were prepared and investigated in two different rubber matrices: Poly(isoprene) [NR] and Poly(styrene-co-butadiene) [SBR].

Experimental

Materials

Rubber grades NR (SMR 5L) and SBR(Buna SB 1500, Schkopau) with 23.5 wt/% of styrene were used as matrix polymers. The microgel types were prepared by emulsion polymerization, subsequent crosslinking and polymer-analogous functionalization as follows.

Poly(butadiene)-microgel, BR(m)

Dicumylperoxide (1-3 wt/%) was added to filtered poly(butadiene) latex while stirring (2 h) at 333K. The emulsion was transfered into an autoclave (Berghof, HR 200) rinsed with nitrogen and heated to 423K for 45 min. in order to avoid coagulation. After crosslinking the latex was slowly added to a stirred, saturated NaCl solution at 333K. The coagulate was filtered off and washed with demineralized water and then with acetone. Finally the material was extracted in a Soxhlet (3 d) and dried in a vacuum.

Poly(styrene)-microgel, PS(m)

An emulsion of styrene and divinylbenzene (ratio 9:1) in bidistilled, degassed water was prepared using $NaHCO_3$ as a buffer and, where necessary, sodium dodecyl sulfate as emulsifying agent in a 250 ml three-necked flask equipped with a KPG stirrer, contacting thermometer and Anschütz set with Reflux condenser and dropping funnel with gas inlet. Polymerization was started by adding a $K_2S_2O_8$ solution (3% in water). Stirring continuously, the mixture was allowed to react for 8 h at 343K. The weighted-in quantities are controlled by the set particle size (Tab. 1). The emulsion is reprocessed by filtering off the coagulate and removing monomer residues through steam distillation. A small amount of hydroquinone is added during the cooling process. Having cooled down to room temperature, the latex is slowly poured into the twice volume of hot, concentrated NaCl solution. The coagulate is filtered off, rinsed with 1 L of demineralized water and 1 L of acetone, and subsequently dried in the water jet vacuum at 313K until constant weight is attained.

Particle size (nm)	H_2O (g)	Styrene (g)	m-DVB (g)
30	100	0,9	0,1
60	100	1,8	0,2
100	100	3,6	0,4
200	100	1,8	0,2
300	100	3,6	0,4
400	100	5,4	0,6
500	100	7,2	0,8

Table 1: Quantities of monomers and water used and the resulting particle size (initiator (0.051 g), emulsifier (0.029 g) and buffer (0. 14 g) are kept constant)

Poly(bromobutadiene)-microgel, Br-BR(m)

BR(m) was swollen in trichloromethane (1 g/ 100 mL) for 2 h. The suspension was cooled to 273K and the appropriate amount of bromine dropped as trichloromethane-solution (1.1 mol/L) under N_2. The suspension was stirred and cooled to 275K during the reaction. After adding the brominesolution the suspension was continuously stirred at room-temperature for 12 h. The suspensions were vacuum concentrated at 303K (or centrifuged) and then poured into methanol to precipitate the microgel. The microgel was filtered, washed with methanol and dried in a vacuum to constant weight. For the determination of the C-, H- and Br-content elemental analysis was employed.

Sample preparation

Blends were prepared by mechanically mixing microgels and raw rubbers on a laboratory two-roll mill at 323 ± 5K. Depending on the purpose variable volume fractions of the particular microgel were incorporated into the rubber. After extensive mixing the crosslinking system consisting of benzothiazolyl-cyclohexylamine and sulfur (ratio 1.5: 0.8) was added. The selection of this curing system assures that only the rubber matrix is cured. Specimens of 200x200x2 mm were press-cured at 433K to the rheometer optimum.

Physical testing

Uniaxial deformations were performed with an universal testing machine (Zwick 1445) equipped with an optical length recorder and a 50N force transducer at a deformation rate of 2 mm/min and a temperature of 293K. The dynamic properties were recorded as amplitude sweeps of G' and tan δ at constant frequency (1 Hz) in the range of 0.01 - 2.5% deformation amplitude with an RDA-700 (Rheometrix) machine. For strain amplitudes up to 100% cylindrical specimens (h=2 mm, d=10 mm) were bonded to steel punches using contactcement. The tests were performed at increasing shearamplitude (0.01 - 100%) and constant frequency (10 Hz) on an MTS-hydropulser 851.50.

Thermodynamic characterization

The solubility parameters of the blend constituents, except Br-BR(m), were determined on uncrosslinked materials by using inverse gaschromatography (IGC). From the retention volumes of n-alkane probes on the particular polymer phase deposited onto chromosorb W-HP in packed GC-columns the polymer-solvent interaction parameters χ_{12} were derived accordingly [7]. The solubility parameters were determined at the testing temperature from the slope and the intercept of the Guilletplots [8]

$$[\delta^2_1 / RT_c - X_{12} / \nu_1] = (2\delta_2 / RT_c)\,\delta_1 - \delta^2_2 / RT_c \qquad (1)$$

where δ_1 represents the probe solubility parameter, ν_1 is the specific volume.

TEM micrographs

Morphological investigations were performed on ultra-thin cuts (80-100 nm) obtained on a microtome UltraCut FC4E (Reichert-Jung). Electron-Spectroscopy-Imaging-Transmission-Electron Microscopy (ESI-TEM) was employed to obtain micrographs on an EM 902 (Zeiβ) machine by filtering inelastically scattered electrons. Due to the contrast achieved supplementary staining of the samples was not necessary.

Results and discussion

Blend morphology

Contrary to blends formed by mechanically mixing two raw rubbers and having a phase morphology that depends not only on the interfacial tension but also on processing conditions [9], the mechanical incorporation of microgels into a rubber matrix (NR or SBR) delivers a dispersion of separated microgels in that matrix without any indication of the particle fracture one would expect considering the high shear forces in internal mixers (Fig. 1).

Due to the extensive mixing of the compounds it can be assumed that the microgel particles are quite welldispersed even at the higher volume fractions, ϕ. At low concentrations, the microgel particles are almost separated from one another in the rubber matrix in a welldispersed state. However, if a critical value of ϕ^+ is exceeded individual aggregates can be observed in all systems investigated. It has to be assumed that once shear forces have been set during mixing, the microgels tend to aggregate if the interparticle interactions with re-

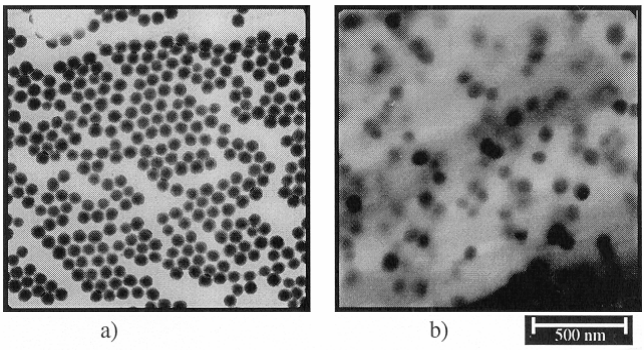

Fig.1: Morphology of a microgel containing elastomer
a) initial sate PS(m);
b) PS(m)/NR at F=0,15

spect to interfacial free energy are more beneficial than the microgel-to-matrix interactions. The higher the interfacial free energy, the higher the critical interparticle distance, too, because the merging of microgel particles to larger clusters is then more readily promoted by the energetic balance than it would be with systems having a low interfacial tension. Because the process of sticking together of neighboring microgel particles takes place primarily after the mixing stage one can employ a kinetic cluster aggregation model to describe the overall evolution in the uncured mix. However, the final morphology is fixed by chemically crosslinking the system.

In accordance with these considerations an obvious tendency towards cluster formation was observed by increasing ϕ and reducing the microgel particle size. It was also shown that cluster formation is supported by increasing the δ-parameter difference in the sequence of the systems PS(m)/SBR($\Delta\delta$=2.18 $(J/cm^3)^{0.5}$), PS(m)/NR ($\Delta\delta$= 3.31), Br-BR(m) [9 mol./%]/ NR($\Delta\delta$=1.18) and Br-BR(m)[33 mol./%]/NR($\Delta\delta$=2.57).

Heterogeneity originates not only from the different chemical constitution of the microgel and the rubber matrix, but also from an increasing state of crosslinking regardless of the polarity of the microgel and consequently the state of clustering, the morphology of stressed elastomers containing weakly crosslinked microgels projects clearly the state of local extension (Fig. 2). In such systems the microgels act like strong elastic springs capable of storing additional stress energy if they are subjected to large strain. Nevertheless, a limit is reached if the local stress exceeds the interfacial bonding energy. The occurring detachments in the top-stress region contributes to the initiation of the catastrophic cut growth in the material.

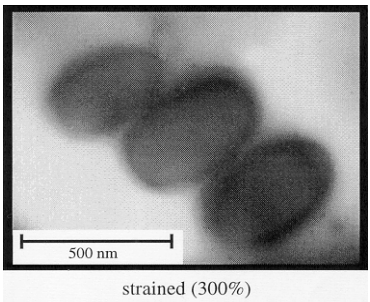

Fig.2: Local deformation of weakly crosslinked BR(m) in NR

Young's modulus

Much insight into the physical behavior is provided by the comparison of the Young's modulus for systems with different interfacial tension between microgel and the matrix if f is increased. The vulcanizates obtained by dispersing PS(m) of particle size ranging from 30 to 500 nm at $\phi \leq 0.25$ in SBR show an increase in the Young's modulus measured at elonga-

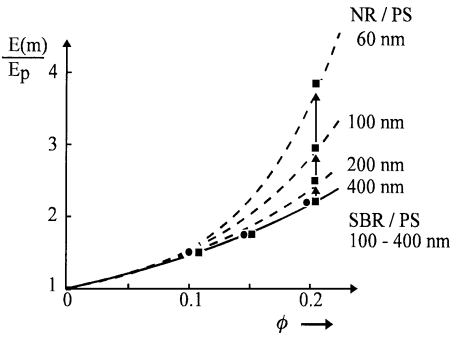

Fig.3: Reinforcing effect of PS(m) in SBR (•) and in NR (■)

tions < 5% (Fig. 3, solid line). The reinforcement of the elastic modulus as a function of the microgel volume fraction strictly obeys the hydrodynamic theory of Smallwood-Guth-Gold [10, 11], which does not assume a strong interaction between the domains of the dispersed phase

$$E_m = E_p(1 + 2.5\phi + 14.1\phi^2 + ...) \qquad (2)$$

where E_p is the Young's modulus of the crosslinked rubber matrix and E_m the Young's modulus of the microgel containing system.

In contrast to this the system PS(m)in NR demonstrates a large positive deviation of the Young's modulus (Fig. 3, dashed lines), which indicates an additional hydrodynamic contribution for which no provision is made by the Smallwood-Guth-Gold-theory. The effect can be related to the pronounced cluster formation tendency of the microgel particles if the particle size is decreased and at the same time poor microgel-to-rubber interactions are compensated for by strong interparticle interactions. By this a critical aggregation limit ϕ^+ is reached, above which individual clusters are formed.

In this region the mechanically effective volume fraction ϕ_{eff} is a function of the solid fraction of the microgel clusters ϕ_A and replaces ϕ in Eq. 1.

$$\phi_{eff} = \phi / \phi_A \qquad (3)$$

The quantity ϕ_A is increasing according to power law with respect to the net concentration $(\phi - \phi^+)$ [12]

$$\phi_A = \left[1 + \beta'(\phi - \phi^+)^B\right]^{-1} \qquad (4)$$

The two parameters β' and B are empirical constants that can be estimated by applying Equs. (2) - (4) together with the experimental values for the moduli entering eq. (1). The critical concentration ϕ^+ (aggregation limit) can be related to a critical diameter d^+ between the filler particles. By using a simple cubic lattice relation between the size a of the microgels and the interparticle distance d^+ it follows:

$$\phi^+ = \frac{\pi}{6}\left[a/(d^+ + a)\right]^3 \qquad (5)$$

It is assumed that the critical distance d^+ depends on the mean spacing of physical chain entanglements in the rubber matrix [12] as well as the interfacial tension [13]. By plotting the related Young's modulus $E(m)/E_o$ at $\phi = 0.2$ as a function of the diameter a of PS(m) in NR and SBR respectively the limit below of which cluster formation starts became obvious (Fig. 4). The results are a = 350 nm in NR and a = 150 nm in SBR. According to eq. (5) the critical mean interparticle distance d^+ at which clustering starts is $d^+ \approx 30$ nm for PS(m)/NR and $d^+ \approx 60$ nm for the PS(m)/SBR. The ranking of these values is a

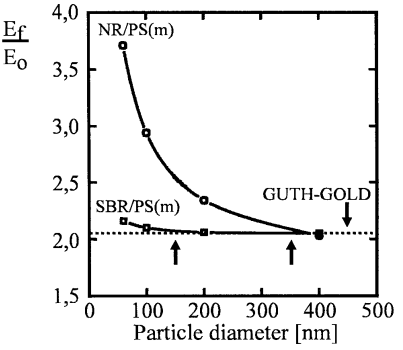

Fig.4: Increase of the related Young's modulus as a function of particle size a (critical diameters indicated by arrows)

projection of the δ-parameter difference of the corresponding blend constituents. From the data for PS(m)/NR the cluster growth function (eq. 4) was calculated for ϕ = 0.2. A least square fit yields β = 362 and β = 3.7, which is in excellent aggreement with theoretical expectations [12]. Further proof that the reinforcing effect is attributable to the aggregation of the microgel particles and that this process is determined by the opposed balance of microgel-matrix interactions and the interparticle interactions, can be seen for BR(m) and Br-BR(m). Because of the low interfacial tension BR(m) do not lead to an increase in the Young's modulus, even at ϕ = 0.33 in SBR. Obviously, in addition a rigidity condition for the microgel particles has to be fulfilled. Weakly crosslinked BR(m) deliver an additive contribution to the mechanical behavior which depends besides the ϕ^+ on their crosslinking density. The mechanical contribution of weakly crosslinked BR(m) can be described by empirical models of coupling and transfer of impulses frequently used to explain the behavior of rubber blends [14]. By comparison, with highly brominated Br-BR(m) (36 mol/%) having a much larger δ-parameter difference and a higher T_g, a reinforcing effect is observed which can only be explained by a high fraction of aggregated microgels (Fig. 5). Reinforcement over and above that given in Eq. (1) is only visible at ϕ = 0.15 once the degree of bromination has exceeded 20 mol/%. With the reduced interparticle distance d^+ at ϕ = 0.33 a 4 to 6 times higher Young's modulus can already be observed at low degrees of bromination (Table 2).

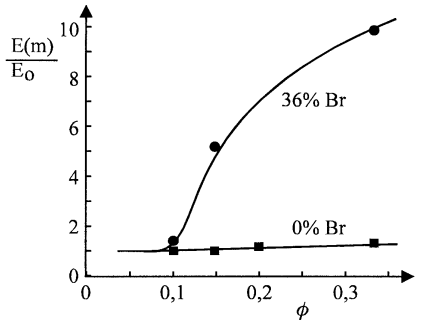

Fig.5: Related Young's Modulus vs ϕ for BR(m) and Br-BR(m) in SBR

ϕ	Br(%)	E(m)/E_o
0.15	10	1
0.15	20	2
0.33	10	4.2
0.33	16	6

Table 2: Effect of bromination on Young's modulus for Br-BR(m)/SBR

Dynamic storage and loss moduli

For all systems investigated at $\phi > \phi^+$ the hydrodynamic reinforcement causes also an increase of the storage modulus G' at small strain amplitudes (SA) of < 0.1 %. It is characteristic for systems with a moderate microgel content that G' is not affected by the increase of strain amplitude (Fig. 6 curve at ϕ=0.2). Obviously the clusters formed at ϕ^+ are not destroyed by the dynamic excitation. The decrease of G' at high SA (> 20%) is attributed to a molecular slippage of the chains on the microgel surface and in the matrix as well.

By increasing the microgel content considerably above ϕ^+ a critical concentration ϕ^* is reached at which G' increases sharply to values which cannot be achieved by reasonable solid fractions of aggregates ϕ_A. The threshold ϕ^* which is typically in the region of 0.35-0.45 is shifted to higher values if the interfacial tension is lowered (Fig.7). The increase of G' at very low strain amplitudes is strongly supported by the increasing degree of surface funtionalization and the decrease of the particle size as can be shown by Fig. 8. By increasing the Br-content from 13 to 34 mol./% in the Br-BR(m) the G' by a factor of 3 whereas at constant Br-content the reduction of the particle size from 400 to 100 nm causes a considerable less increase of G'.

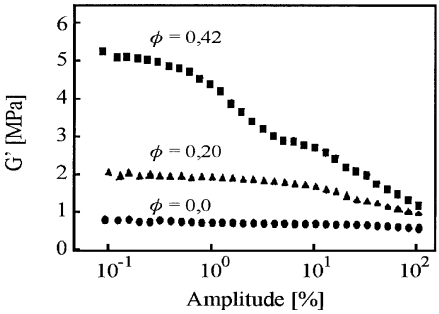

Fig.6: G' vs. SA for BR(m)/NR (10Hz)

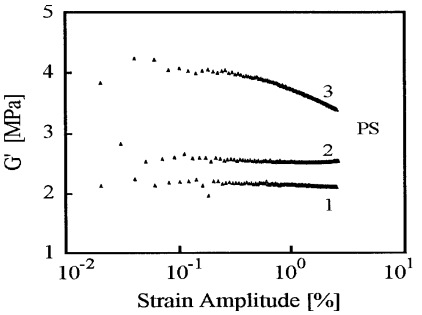

Fig.7: G' vs. SA at 10Hz for 1) PS(400)/NR; 2) PS(60)/SBR; 2) PS(60)/NR

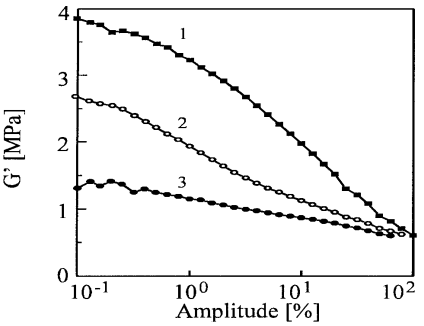

Fig.8: G' vs. SA for Br-BR(m)/NR; 1) 400 nm, 34 mol% Br; 2) 100 nm, 15 mol% Br; 3) 400 nm, 13 mol% Br

A characteristic feature of all these systems at $\phi > \phi^*$ is the pronounced decline of G' if the SA is increased above 0.5 %. The bimodal curves G' vs. strain amplitude indicate the existence of two distinct regions. The first region ranging from 0.5-1.0% up to 2-5% SA is commonly observed also for elastomers filled with carbon black or silica [15]. Therefore the decline of G' from G_o' at very small SA to G_∞' at very large SA (see Fig. 6 to 8) demonstrates an universal behavior of rubber networks highly filled with colloidal particles. The second region corresponds in our opinion to chain slippage. The comparison (Fig. 6 to 8) shows that the value of SA at which G_o' starts to decline is shifted towards higher SA if surface functionalization becomes more pronounced and can result in an overlap of both regions (see 34 mol./% Br-BR(m)/NR, Fig. 8). The key phenomenon is the formation of throughgoing three dimensional microgel networks above the gelification point ϕ^*. The structure of these corresponds to that of the spacefilling configurations of cluster-cluster aggregations (CCA) [12,16]. An important feature are the predicted universal power laws of the small-strain modulus G_o' of the compound

$$G_0^{'} \cong G(m)\left(a/\xi\right)^3 N_B(\xi)^{-1} \cong G(m)\left(a/\xi\right)^{3+d_{f,B}} \qquad (5)$$

$$G_0^{'} \cong G(m)\,\phi^{(3+d_{f,B})/(3-d_f)} \qquad (6)$$

where G(m) denotes the storage modulus of the microgels, a is the particle size, ξ is the size of the CCA-cluster (correlation length), N_B is the number of particles in the cluster backbone, d_f is the fractal dimension of the CCA-cluster ($\approx$ 1.8), $d_{f,B}$ is the fractal dimension of the CCA-cluster backbone that relates the particle number N_B to the correlation length ξ ($\approx$ 1.3). Eq. (5) assumes that the small-strain modulus of highly concentrated elastomers can be appoximated by the modulus of the microgel, which determines the modulus of the througoing network that in turn equals the modulus of the CCA-clusters of size ξ. Furthermore, due to the homogeneity of the three-dimensional microgel network on large length scales (>>ξ) G_o' equals the modulus of a single cluster and is independent from that of the rubber matrix. Eq.

(6) predicts that G_o' depends only on the concentration $\phi > \phi^*$ with an exponent of $(3 + d_{f,B})/(3 - d_f) \approx 3.5$. This is in agreement with experimental findings.

Because clusters broken during dynamic deformation cannot transmit stress between the remaining neighboring clusters in the throughgoing network a percolation lattice model can be used to derive the strain amplitude dependency of G'(γ). The fraction P(γ) of sites occupied by clusters equals the ratio between the number N(γ) of CCA-clusters at given strain γ and the initial number N_0 in the throughgoing network

$$P(\gamma) = N(\gamma) / N_O \tag{7}$$

The number of surviving clusters N(γ) can be modelled by a rate equation, that considers an equilibrium between broken and aggregated clusters within each deformation cycle [17]. Considering the strain amplitude, where half of the clusters are broken $\gamma_{1/2}$ and the critical occupation number P_c where the percolation network is formed the decline of G'(γ) can be expressed by a function of the Havriliak-Negami-type

$$G'(\gamma) \cong G_0' \left[1 + (\gamma / \gamma_{1/2})^{\alpha}\right]^{-\tau} \tag{8}$$

where τ is the elasticity exponent (≈ 3.6) and a an empirical parameter.

According to this equation which fits fairly well with the experimental findings at small strains the major part of interparticle interactions survive during the initial drop of G'(γ) by means of sub-clusters that break down at significantly larger strains.

References

[1] Bischoff A, Hallensleben ML, Schuster RH 2nd Internat. Sympos. "Polymer for Advanced Technologies" (PAT '93) Sept. 1993
[2] Bischoff A (1992) Thesis University Hannover
[3] Nuyken O, Bayer R (1995) Kautsch. Gummi Kunstst. 48:704
[4] Nuyken O, Ko SK, Voit B, Yang D (1996) Kautsch. Gummi Kunstst. 48:784
[5] Witten TA, Rubinstein M, Colby RH (1993) J. Phys. II (France) 3:367
[6] Meakin P (1990) Prog. Solide State Chem. 20:135
[7] Patterson D, Tewari YB, Schreiber HP (1972) J. Chem. Soc. Faraday Trans. 2, 68:885
[8] Smidsrod O, Guillet JE (1969) Macromolecules 2:279
[9] Schuster RH, Issel HM, Peterseim V (1996) Rubber Chem. Technol. 69:769
[10] Guth E, Gold O (1938) Phys. Rev 53:322
[11] Smallwood HM (1944) J. Appl. Phys. 15:758
[12] Klüppel M, Heinrich G (1995) Rubber Chem. Technol. 68: 623
[13] Schuster RH, Klüppel M, Früh T (submitted) Rubber Chem. Technol.
[14] Taganayaki M, Uemura S, Miami S (1964) J. Polym. Sci. PAT C, 5:113
[15] Payne AR (1962) J. Appl. Polym. Sci. 6:57
[16] Klüppel M, Schuster RH, Heinrich G (1997) Rubber Chem. Technol. 70:243
[17] Kraus G (1984) J. Appl. Polym. Sci., Polym. Symp. 38:75